

Effects of climate change on wind energy production in Iran

Gholamreza Roshan · Mohammad Saeed Najafei ·
Ángel M. Costa · José A. Orosa

Received: 18 September 2013 / Accepted: 12 March 2014 / Published online: 27 March 2014
© Saudi Society for Geosciences 2014

Abstract This study explores the effect of future climate change on wind energy conversion in Iran, based on data from existing wind farms. In an effort to estimate and understand the effects of climate change on the potential of wind energy production, the southwestern and western regions of Iran have been studied. In this region, the three provinces of Ilam, Kermanshah and Khuzestan have been studied in detail, along with their 12 weather stations. To simulate future temperatures, the HADCAM3 general circulation model and A1b and A2 scenarios were used. The method of artificial neural network (ANN) was deployed to predict the measures of relative humidity. To compare the rate of energy production for the two periods of present and future conditions, two time scales, 1987–2009 and 2046–2065, were taken into account. The main results demonstrate that there is an agreement between the two future climate scenarios, A1b and A2. In both simulations, Dehloran City showed the highest moist air density and, consequently, the highest wind energy production. In the other cities, a decrease in wind energy production was observed. Finally, if the mean working life of a wind farm is assumed to be between 20 and 30 years, the more promising regions in which to implement and/or renovate wind farms, in Iran, can be determined, according to the expected future wind energy production. The research further indicates an increase in temperature in most of the stations in the months studied

and a decrease in the capacity of wind energy production in most stations. Therefore, a lack of proper management of supply and a demand of energy for cooling and ventilation of settlements in the studied regions can lead to challenges in providing the society with healthy climatic conditions in that area. Thus, a proper alternative, such as solar energy, to supply the region with clean energy is proposed.

Keywords Climate change · Wind energy · Moist air · Density

Introduction

Subsequent to hydropower, at present, wind turbines and thermal power based on biomass are the two most developed and cost-effective renewable electricity production technologies (Hu et al. 2013; AL-Yahyaia et al. 2014). As a result, a significant growth in installed wind power capacity has occurred in Germany, Spain, Denmark and China in recent years (Hu et al. 2013). Large-scale introduction of wind turbines as a power system will influence the day-to-day operation of electricity production, as also the future development of the portfolio of power plants and transmission lines within the power system (Meibom et al. 2009).

New methods in wind energy conversion have been developed in the last few years. For example, in regions with low wind speed, like India, wind concentrators have been developed (Sabzevan 1977; Frankovic and Vrsalovic 2001; Shikha et al. 2003; Shikha et al. 2005).

However, an in-depth analysis has not been undertaken on future viability of these power options, including the effect of climate change on wind energy conversion. Hence, this study explores the effect of future climate change on wind energy conversion in Iran, based on real sampled data from the existing wind farms.

The demand for primary energy in Iran is projected to increase at an average annual rate of 2.6 % during the period

G. Roshan (✉)
Department of Geography, Faculty of Human Science, Golestan
University, Shahid Beheshti, Gorgan 49138-15759, Iran
e-mail: ghr.rowshan@gmail.com

G. Roshan
e-mail: ghr.roshan@gu.ac.ir

M. S. Najafei
Department of Geography, University of Tabriz, Tabriz, Iran

Á. M. Costa · J. A. Orosa
Department of Energy, M.P. University of A Coruña, Paseo de Ronda
51, 15011 A Coruña, Spain

2003–2030, with an increase of 5 % over the past decade (Najafi and Ghobadian 2011). Renewable energy resources do not have wide applications in Iran at present, as most of the energy is supplied by fossil fuels (Fig. 1). These renewable energies, especially wind energy, will enable Iran to obtain electricity more easily from nonfossil energy sources and will consequently decrease the consumption of fossil fuels.

Iran has a great potential for improving energy services through renewable sources, but at present, only about 0.04 % of its electricity is generated from the wind (Fadaia et al. 2011).

Iran's first experience in installing and using modern wind turbines was initiated in 1994. Two sets of 500-kW NORD-TANK wind turbines were installed in Manjil and Roodbar. Together, they produced more than 1.8 million kWh/year. These two sites are in the north of Iran, 250 km from the capital Tehran. The average wind speed is 15 m/s for 3,700 h/year in Roodbar and 13 m/s for 3,400 h/year in Manjil. After the success of this operation, a contract for 27 wind turbines was signed in 1996, and installed by 1999, in Manjil, Roodbar and Ardebil. Ardebil is the third wind farm site close to Manjil. Manjil is about 800 masl and Ardebil is about 500 m higher (Mostafaeipour and Abarghoeei 2008). In addition, assessments of the wind energy potential in Iran have been carried out for numerous locations, such as Semnan (Mirhosseini et al. 2011), Manjil (Dehghan 2011) and Yazd (Mostafaeipour and Abarghoeei 2008).

For example, in 2007, data on 68 stations were analysed to determine the general characteristics of the wind energy potential. The wind speed distribution was calculated at 10, 20, 30 and 40 m above ground level, in Iran, using geographic information system (GIS) interpolation techniques. It was concluded that the eastern and northwestern regions of Iran had a good potential for wind power, while the central and southern regions had a much lower potential for grid-connected wind energy installation (Alamdari et al. 2012). Keyhani et al. (2010) used wind speed measurements of

11 years, for the capital of Iran, Tehran, to identify the wind energy potential. The results revealed that the highest and lowest wind power potentials were in April and August, respectively, and it was concluded that the site studied was not suitable for electric wind application on a large scale (Keyhani et al. 2010).

There are also studies about the feasibility of offshore wind turbine installations in Iran, in comparison to the rest of the world (Mostafaeipour 2010).

Analysing the statistics published by the World Wind Association, Najafi and Ghobadian (2011) argue that Iran had a wind power capacity of 130 MW in 2009 and was ranked 38th in the world. Another study demonstrated that the potential capacity of wind power for Iran was around 6,500 MW, predominantly in the eastern regions (Mostafaeipour et al. 2011; Ghorashi and Rahimi 2011). In recent times, the Renewable Energy Organization of Iran provided a map using 100 wind speed measurement instruments distributed around the country, for tentative wind energy, demonstrating 45 suitable sites in Iran 0.

With regard to the weather conditions, the southwest of Iran (Khouzestan Province) has a warm and sultry climate, and during the warm days of the year (spring and summer), these conditions are intensified. Due to the high air pressure in the Azores and the upper atmosphere of Iran, the heat of summer affects many regions of the country, particularly the western regions (Ilam and Kermanshah Provinces), and during this period, a very hot and dry weather is dominant. Under continued global warming, Iran is projected to experience warmer temperatures than at present (Roshan et al. 2010, 2011, 2013a; Roshan Gh and Grab 2012). This will likely result in a greater demand for energy for the ventilation and cooling of establishments, especially in the summer season. To tackle this problem, crisis management should be replaced by risk management and planning in the field of energy supply. With regard to the global warming effect, this research explores the changes which will occur in the rate of the wind energy potential of the studied region in the future decades. Taking into consideration the future climate change, it is important to determine whether the capacity of wind energy production will increase—making this a viable solution—or whether the capacity of wind energy production will decrease, in which case we will be faced with new challenges in energy supply in the studied region.

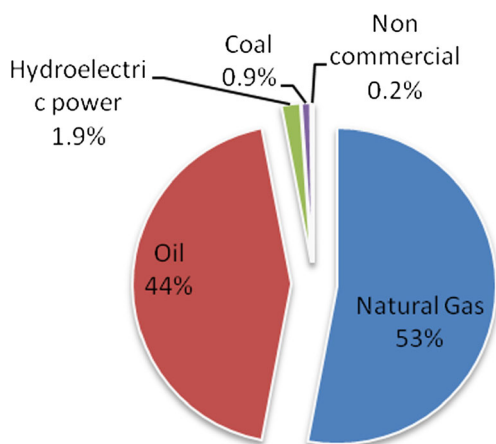


Fig. 1 The total of different types of energy consumption in Iran (EIA 2009; WWEA 2009; Gas Journal and as of January 2010)

The study area

Iran is located in the west of Asia, in the belt of arid to semiarid regions (Hojati et al. 2011). The mean annual rainfall of the country lies between 224 and 275 mm. The study area includes the three provinces of Kermanshah (45.24–48.30° E; 33.36–35.15° N), Ilam (45.24–48.10° E; 31.58–34.15° N) and

Khuzestan (47.42–50.39° N; 29.58–32.58° N) (Fig. 2 and Table 1). This region comprises 45 cities and a population of more than 4,000,000 people. The topographic elevations in these provinces vary between sea level and 3,701 m (Menar Mountain in Khuzestan Province). The northern regions of the study area experience cold winters and warm summers (especially the mountainous areas). In the mountainous areas, the mean inter-annual minimum temperature in the coldest month, January, is less than $-4\text{ }^{\circ}\text{C}$. The southern parts of Khuzestan Province, especially the low elevations and coastal areas, experience tropical weather. The mean annual mean maximum temperatures in summer reach $50\text{ }^{\circ}\text{C}$ (July), whilst the minimum winter temperature is $9\text{ }^{\circ}\text{C}$ (March) (Najafi et al. 2013).

Materials and methods

Climatic data

In accordance with the methodology developed in previous research studies, climatic data were sampled from weather stations located in the potential locations of wind farms (MeteoGalicia 2007). This included temperature, relative humidity and wind speed, with a sample frequency of about 5 to 10 min. These variables were used to define moist air density. These particular weather stations were selected for this study, as they avoided buildings and other obstructions that could interfere with the sample data, according to the ASHRAE 2005 (ASHRAE 1988) measuring conditions. The margins of error in temperature, relative humidity and wind velocity were $0.1\text{ }^{\circ}\text{C}$, $0.2\text{ }\%$ and 0.1 m/s , respectively.

Table 1 The geographical location and roughness length Z_0 of stations used in this study

Station	Z_0	Longitude	Latitude	Elevation (m)
Abadan	0.09	48' 15" E	30' 22" N	6.6
Ahwaz	1	48' 40" E	31' 20" N	22.5
Bostan	0.1	48° E	31' 43" N	7.8
Dezful	0.09	48' 23" E	32' 24" N	143
Omidiyeh	0.2	49' 39" E	30' 46" N	34.9
Ramhormoz	0.1	49' 36" E	31' 16" N	150.5
Kermanshah	0.61	47' 09" E	34' 21" N	1,318
Sarpol Zohab	0.2	45' 52" E	34' 27" N	545
Eslamabad-e Gharb	0.4	46' 28" E	34' 07" N	1,348.8
Ravansar	0.4	46' 39" E	34' 43" N	1,379.9
Ilam	0.4	46' 26" E	33' 38" N	1,337
Dehloran	0.7	47' 16" E	32' 41" N	232
Behbahan	0.2	50' 14" E	30' 36" N	313

Sotavento wind farm

Sotavento Galicia is a ‘showcase’ of different wind power technologies, which strives to achieve the following goals: to provide framework for carrying out I + D activities; to become a training and debate centre; to be a model centre for developing renewable energies; and to be an exhibition wind farm.

This farm houses 24 wind turbines of five different technologies, with a total nominal power of 17.56 MW and an annual production of 38,500 MW. All of the wind turbines have a horizontal axis rotor, and their wind power conversion begins at 3 m/s. The turbines are disconnected from the electrical network when wind speeds exceed 25 m/s, with predominant winds from the southwest and northwest. All

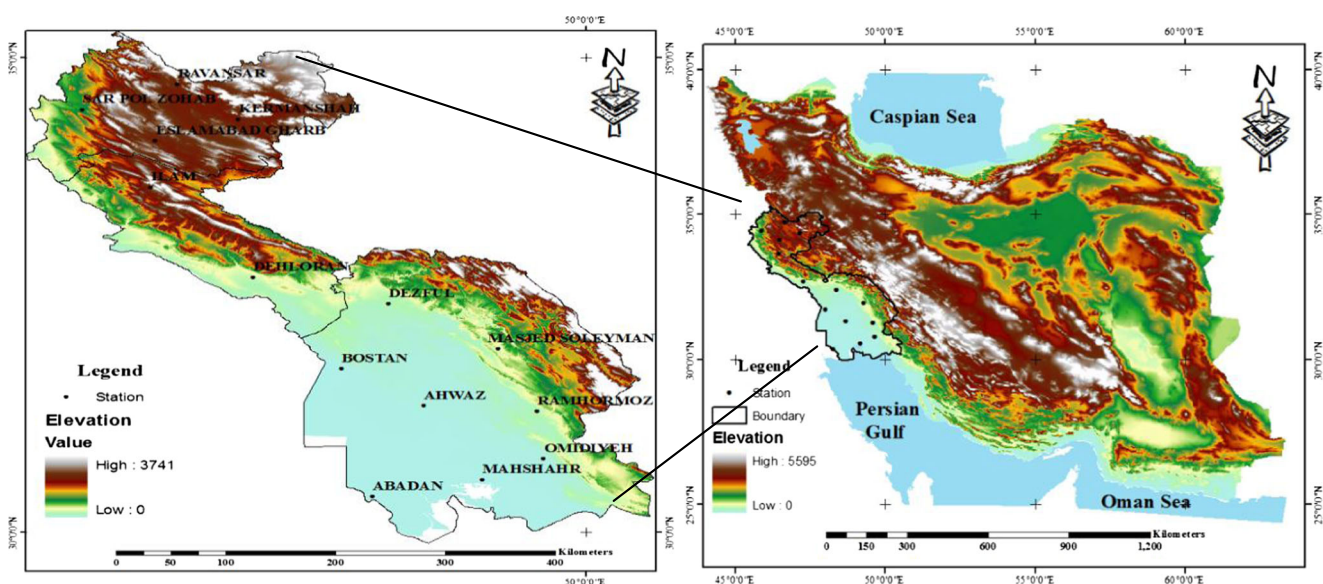


Fig. 2 Distribution of the stations under study in the southwest, west and northwest of Iran

the data concerning the power production is stored in the Sotavento centre and updated at a frequency of 10 min.

Curve fit

Once the annual wind power conversion data were obtained from the wind farms, they were compared with the weather conditions during the same year using the statistical software SPSS.

To develop generic model of wind energy conversion through our wind farm, curve fitting was undertaken using the real sampled data of weather conditions and wind energy production (Fig. 3).

The resulting correlation is given by Eq. (1), with power production varying linearly with air density and with wind velocity cubed. The correlation coefficient of 0.99 is particularly high, confirming the accuracy and statistical significance of the model.

$$P_{\text{HAWT}} = -249,492.18 + 217,222.74 \cdot \rho + 1,128.9655 \cdot V^3 \quad (1)$$

where

P_{HAWT}	Power production in a traditional turbine (kWh)
ρ	Moist air density (kg/m ³)
V	Wind velocity (m/s)

Vertical wind profile

For meteorological applications, wind speed measurements are taken 10 m above the ground. By contrast, wind energy applications require wind speed data at the axial height of the turbine, due to the influence on both the assessment and the turbine design. Wind at higher levels can be calculated using the logarithmic law (Petersen et al. 1997; AL-Yahyaia et al. 2010; Zarghami et al. 2011). This logarithmic law (Eq. (2)) is used to interpolate the wind speed at 65 m.

$$v_2 = v_1 \frac{\ln(z_2/z_0)}{\ln(z_1/z_0)} \quad (2)$$

where v_1 is the known wind velocity at height Z_1 , and V_2 is the predicted wind speed at height Z_2 ; Z_0 is the roughness length at the site of interest. In this study, the roughness length values were derived from the closest grid point of 7 km resolution of the dataset (Table 1).

Downscaling approach in climate change by LARS-WG

As the resolution of general circulation models (GCMs) is low, we cannot yet predict the meteorological output scales as small as a city. To predict meteorological data on small scales, the GCM outputs need to be downscaled using dynamic or statistical models (Zarghami et al. 2011; Awadh and Ahmad 2012; Iqbal et al. 2011).

For statistical downscaling, two datasets are required, the observed data and the output data, of the general atmospheric circulation. For this study, observed data for the period 1987–2009 were used as the baseline period, and the data from the atmospheric circulation model (HADCAM3) under scenarios A1b and A2 were used to project climate changes for the period 2046–2065. The statistical downscaling using the model LARS-WG version 5.11 was thus employed. Model HADCAM3 has been used in the Hadley Centre for Climate Prediction and Research (HCCPR) in England, and it has a differentiation power of 2.5° in latitude and 3.75° in longitude (Roshan et al. 2013b).

A LARS-WG is used for observing daily meteorological data (including minimum temperature, maximum temperature, precipitation and radiation) of a given site, to determine the parameters driving the probability distributions for weather variables, as well as the correlations between them. The procedure that generates synthetic weather data was based on selecting values from the appropriate distributions using a pseudo-random number generator (Semenov et al. 1998).

To validate the results of the simulations, the LARS-WG implements a number of statistical tests, to compare the data that are produced by the weather generator with the observed data of the baseline period. This statistical test includes the standard deviation, T test, F test, correlation coefficient and its p values. This comparison test clearly shows how the downscaling process

Fig. 3 Wind farm power production

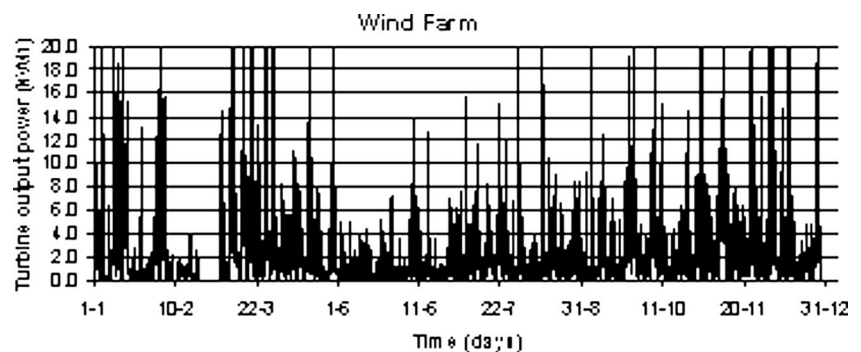
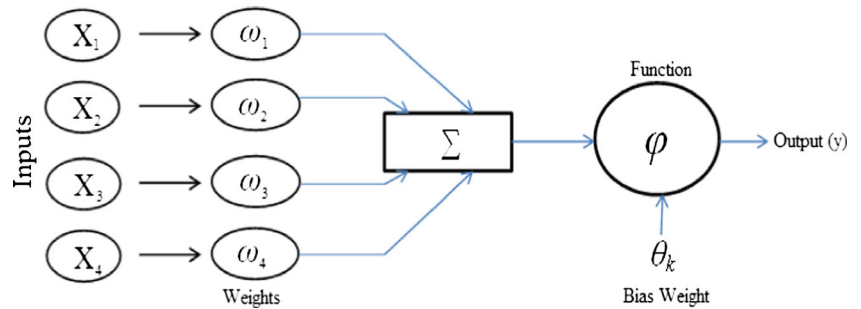


Fig. 4 The structure of the network for estimating relative humidity



reports of the characteristics of the observed data (Zarghami et al. 2011; Roshan et al. 2013c). More details about the LARS-WG model may be found in the relevant literature (Johnson et al. 1996; Semenov and Barrow 1997; Semenov et al. 1998; Babaeian and Kwon 2005; Semenov 2007).

Artificial neural network

In this study, the outputs of the minimum and maximum temperatures, the output temperature and radiation of model HADCM-3, are used to estimate the relative humidity for the period 2046–2065, and based on these, through modelling in the artificial neural networks (ANN), the measures of relative humidity have been simulated. The type of ANN was selected based on the climatological studies (Xu et al. 2012) to multilayered perceptron (MLP) with algorithm back-propagation.

This network was basically considered as a feedforward network, which is taught via the back-propagation model.

Typically, all the units in an MLP feedforward neural network are arranged with three layers that include the input layer, the hidden layer and the output layer. The first layer connects with the input variables, and the last layer connects to the output variables and is of only one unit. The layers in between the input and output layers are called the hidden layers; there can be more than one hidden layer.

Moreover, in the multilayered neural network, based on Fig. 2, the connection between the input elements in the first layer (X_i) and output elements in the last layer (y) is showed with the help of neuron weights (W), bias and membership function (Fx).

The number of units in the hidden layer is an important parameter of the network (Coulibaly et al. 2000; Choobbasti

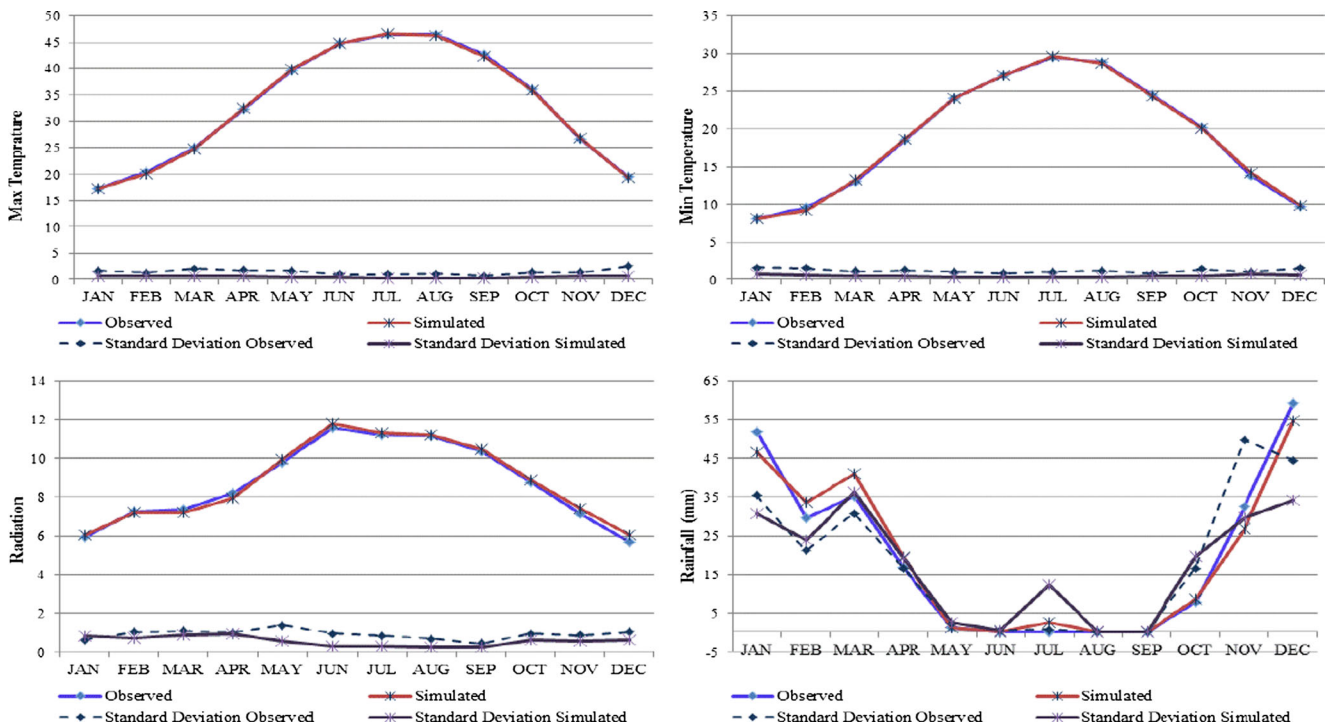


Fig. 5 Comparison of the observed and estimated data in Ahwaz station

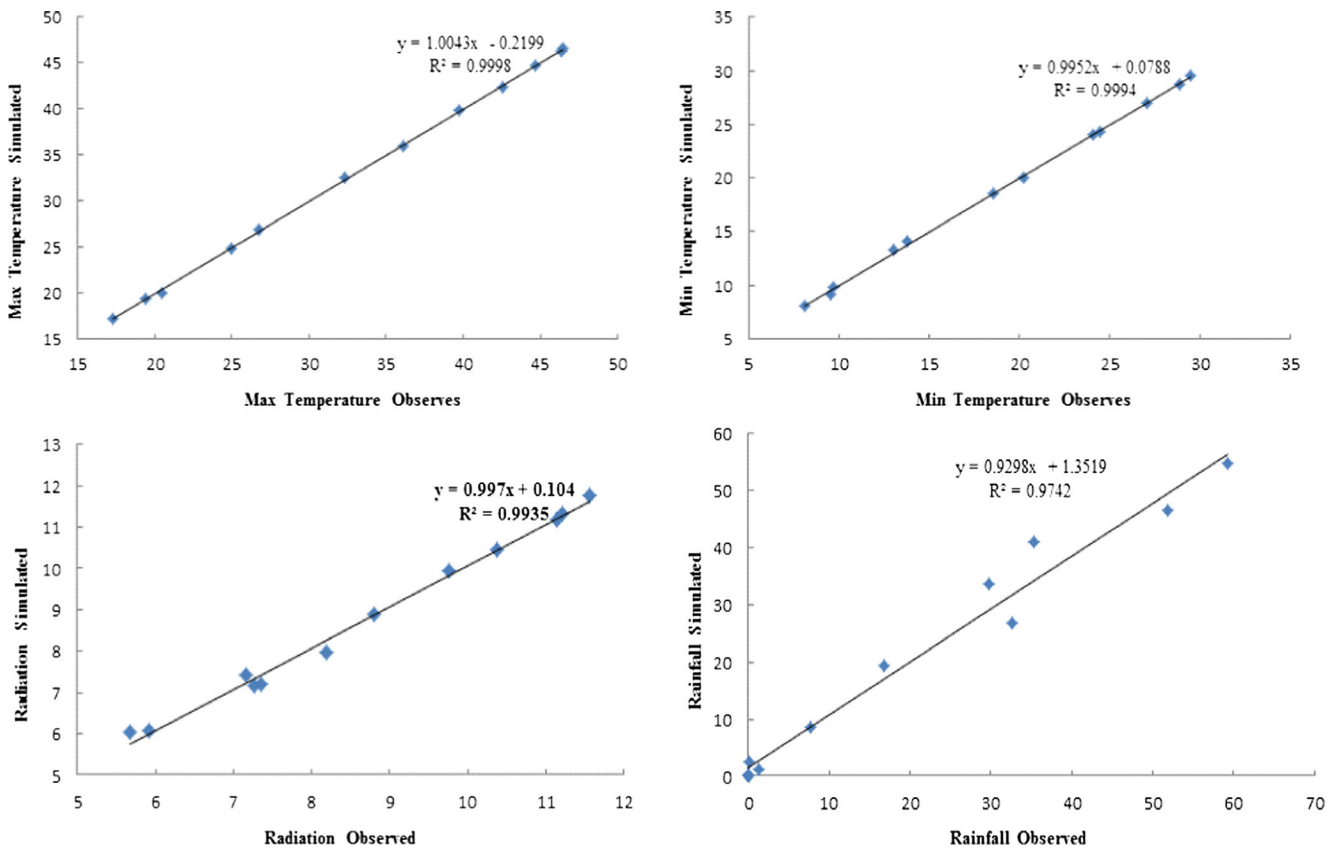


Fig. 6 Scatter plot of the observed and estimated data in Ahwaz station

et al. 2009). The procedure of modelling in ANN consists of three steps.

1. Data preparation: Basically, choosing proper factors as the inputs for the ANN model, for estimating relative humidity, is an important aspect of this approach, as many meteorological factors are related to relative humidity. As the LARS-WG model can estimate only the maximum temperature, minimum temperature, rainfall and daily radiation, we used these variables as the inputs for the ANN model, in this study. The mean coefficients of correlation between relative humidity and input variables in the study area were -0.9 , -0.88 , 0.57 and -0.9 , respectively, which were significant on the level of 0.99 %, in all the stations. The output layer depicts relative humidity in the 2,046–2,065 time series. The datasets for training, validation and test are from 1987 to 2008.

The data, after normalising and being put in the range of 0–1, are divided into three categories: training data (70 %), validation data (20 %) and test data (10 %) (Zare Abyaneh et al. 2009).

2. Model structure selection: The model structure used in this study was a neural network, MLP. The training algorithms for choosing the best algorithm were the Levenberg-Marquardt, momentum, delta bar delta, step,

conjugate gradient and quickprop methods. The sigmoid function was used because of its appropriate operation in modelling the relative humidity.

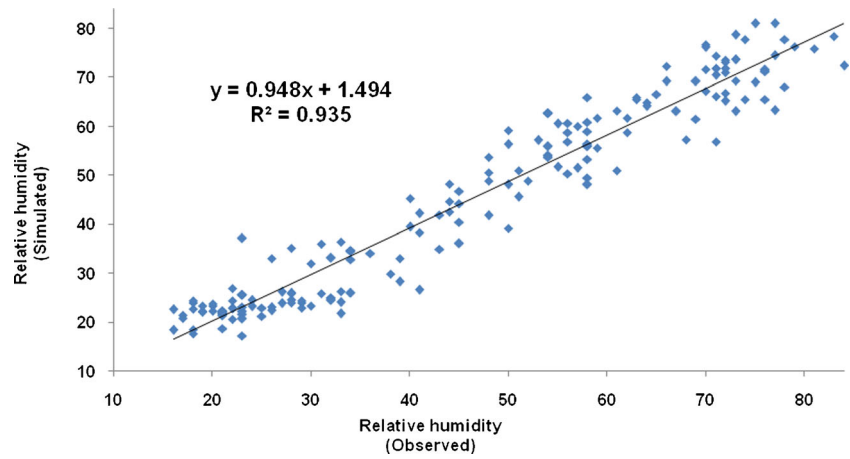
In order to select the best structure, the ANN that had three layers and a different number of neurons for each station in the middle layers was used. The number of presupposed epochs in training the ANN was considered to be 1,000, and the changes in the neurons of the middle layers were one to ten neurons. The standards used for selecting the optimum structure for the artificial neural

Table 2 The performance of network in different training algorithms

Best structure	Algorithm	Validation			
		RMSE train	RMSE test	R^2 test	MAE
5–5–1	LM	0.083	0.086	0.935	0.072
6–5–1	CG	0.115	0.12	0.891	0.081
5–4–1	Momentum	0.116	0.118	0.873	0.093
6–5–1	Step	0.182	0.187	0.796	0.164
6–5–1	Quickprop	0.171	0.178	0.832	0.105
5–5–1	D.B.D.	0.118	0.123	0.884	0.089

LM Levenberg-Marquardt, CG conjugate gradient, RMSEA root mean square error of approximation, D.B.D. delta bar delta, MAE mean absolute error

Fig. 7 Distribution of estimated data of relative humidity in comparison with the observed data



network were the mean absolute error (MAE), root mean square error (RMSE) and determination coefficient (R^2).

$$R^2 = \frac{\sum_{k=1}^k x_k y_k}{\sum_{k=1}^k x_k^2 \sum_{k=1}^k y_k^2} \tag{3}$$

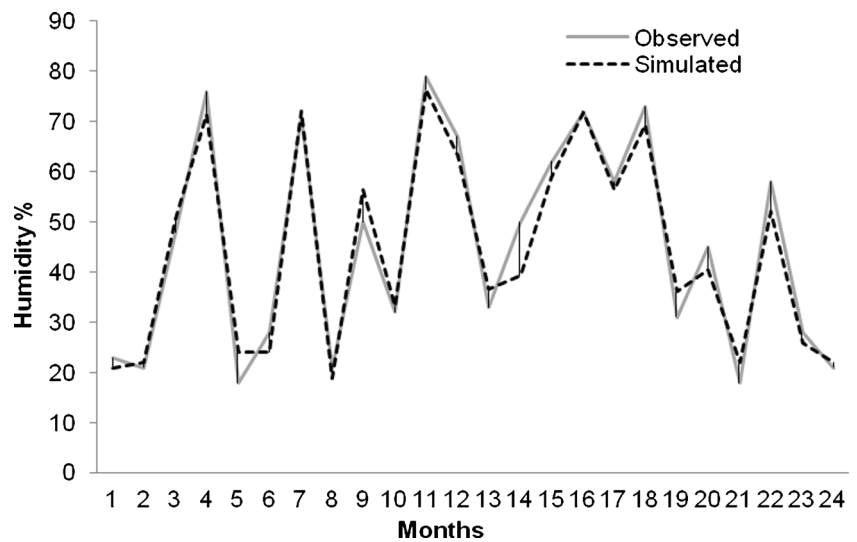
where X_k depicts the observed measures, Y_k the estimated measures and k the number of the data.

$$RMSE = \sqrt{\frac{\sum_{i=1}^n (T_i - Y_i)^2}{n}} \tag{4}$$

$$MAE = \frac{1}{n} \sum_{i=1}^n |T_i - Y_i| \tag{5}$$

In the above-mentioned relations, T_i is the observed measure (objective), Y_i the predicted measure, and n the number of the patterns (Fig. 4).

Fig. 8 Comparison of the observed and estimated mean relative humidity with ANN in the study area in the years 2007 and 2008



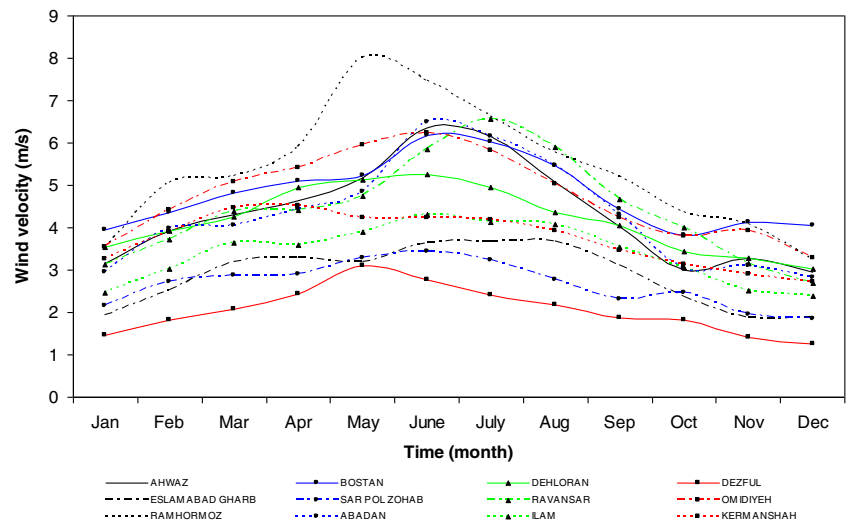
3. Model validation: This step includes a graphical comparison between the simulated and observed outputs. If the training result is not satisfactory, then we change the number of units in the hidden layer or change the functions from the input layer to the hidden layer and then retrain the network again (Huang et al. 2007). The software used in this study for processing ANN is the Neuron Solution 6.

Results and discussion

The validation of the LARS-WG

Since there are a lot of stations and we are not able to present all in the article, the output validation of the simulated and observed data is presented in Figs. 5 and 6, only for the Ahvaz station. As the output shows, the model has an acceptable performance in simulating the minimum and maximum temperatures, radiation and rainfall. Although the simulation of

Fig. 9 Wind velocity in the different cities



the rainfall measures does contain some small errors, we can consider it as the high variation coefficient of rainfall in this area of Iran. Evaluating the absolute error of the simulated data for the parameters of the minimum and maximum temperatures, radiation and rainfall includes 0.2, 0.7, 0.8 and 1, respectively, which indicates the appropriate capability of the model for simulating the data in the baseline period. The correlation coefficient between the minimum and maximum temperatures, rainfall and radiation has been calculated, and the observations have been worked out to be, 0.999, 0.999, 0.996 and 0.98, which are indicative of the fact that this test is meaningful for all parameters at a certainty level of 99%. Finally, the statistical Student's *t* test values for the parameters of minimum and maximum temperatures, rainfall and radiation were 0.2, 1.54, 0.02 and 1.68, and the *p* values for these have been evaluated to be 0.84, 0.14, 0.98 and 0.11.

The validation of the model of the artificial neural network

The results of the application of the introduced ANN structure for estimating the relative humidity in different modes of functions and the number of neurons in the first and middle layers show that the best structure for predicting the relative humidity is the three-layered structure, with five neurons in the hidden layer, and the training algorithm LM (Table 2). The determination coefficient between the simulated data and the real data in the best performance is 0.935, and the training error is 0.083. The final output of the model for validation of the simulated data of relative humidity in relation to the observed data for the whole area under study has been shown in Figs. 7 and 8.

At present, the wind velocity has shown its highest values in the months of June and July in nearly all the cities, as we can see in Fig. 9. At the same time, the lowest wind velocity is

Fig. 10 Air temperature in the different cities

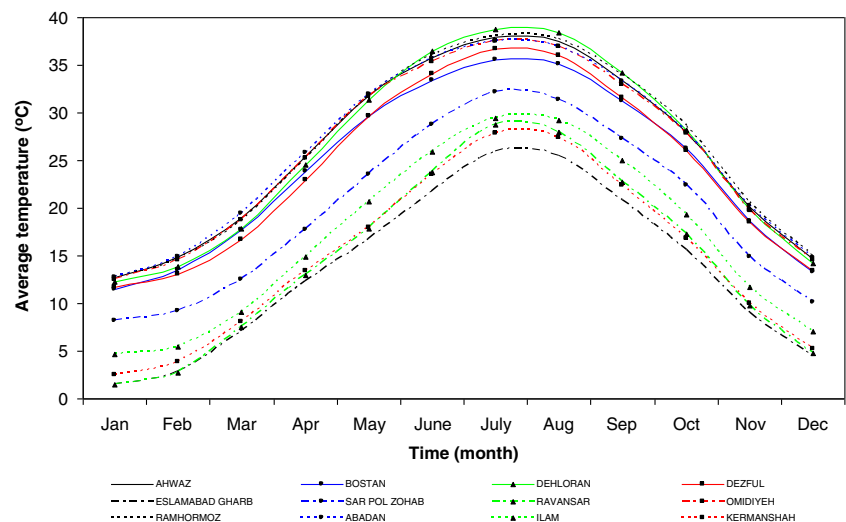
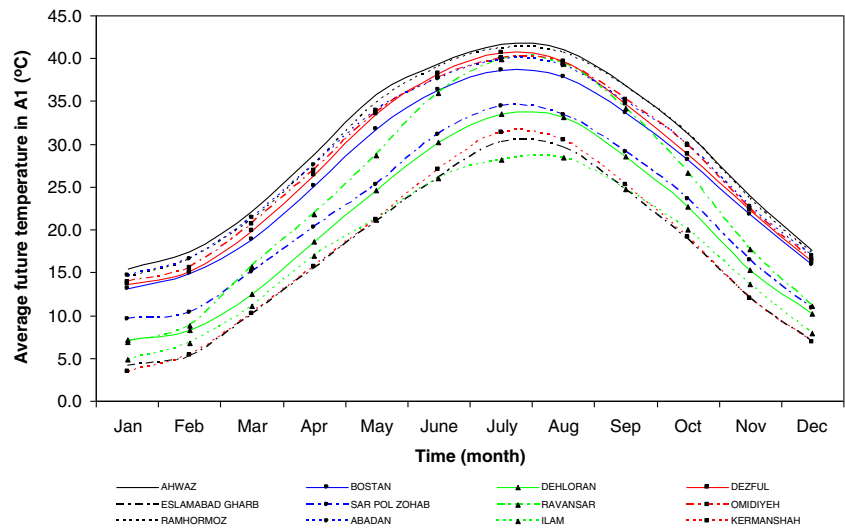


Fig. 11 Air temperature prediction in the A1b scenario



obtained in the month of December. In particular, Ramhormoz is the city with the highest wind velocity and Dezful is the city with the lowest wind velocity, reaching values below the minimum conditions needed to work the wind turbines.

On the other hand, the months of July and August have the maximum temperatures and the month of January has the minimum temperature, as can be seen in Fig. 10. In particular, the highest temperature values were obtained in the city of Dehloran, and the minimum in the city of Eslamabad Gharb, with values of 2 °C.

When future conditions, in accordance with the A1b scenario, are analysed, a clear increment of air temperature is obtained, as can be seen in Fig. 11. As a consequence, there is a decrement in moist air density, as shown in Fig. 12, and a reduction in wind energy production is expected, in accordance with Fig. 13. The cities of Ahwaz and Ilam, in particular, show the maximum and the minimum values, respectively.

As a consequence of this, there is an increment of moist air density of only 2.0 % in the city of Dehloran and a clear decrement in the other cities, with an average decrement of 0.6 %, more particularly in the city of Ravansar, which shows a decrement of 4.0 %.

Accordingly, the city of Dehloran showed the highest wind energy production of about 10 % with respect to the actual conditions. On the other hand, the other cities showed a decrement of 10 %, except the city of Dezful, which showed the highest decrement of wind energy production, as can be seen in Fig. 13.

When the A2 scenario was analysed, it was observed that nearly the same temperatures were predicted for the same cities. The same was the case with the maximum temperature in the city of Ahwaz. Despite this, a slight variation was obtained in the expected minimum temperature, which related to the city of Ravansar in the month of January, as Fig. 14 shows.

Fig. 12 Increment of air temperature in the A1b scenario

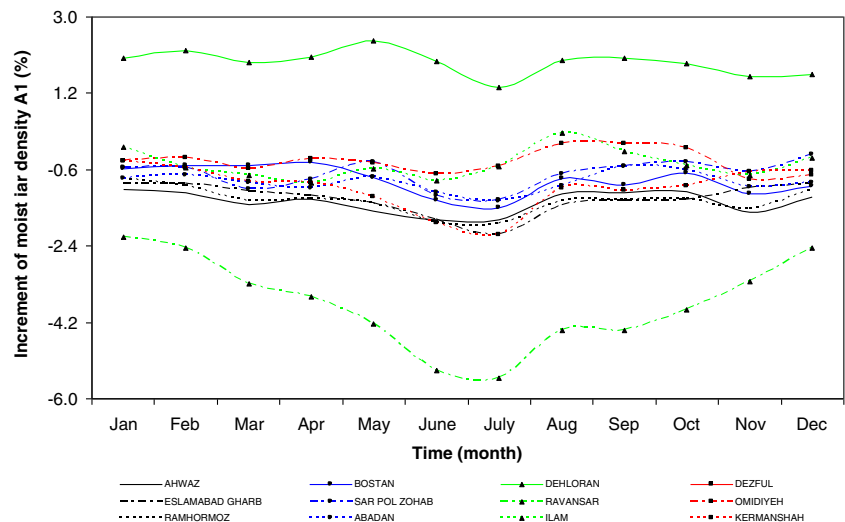
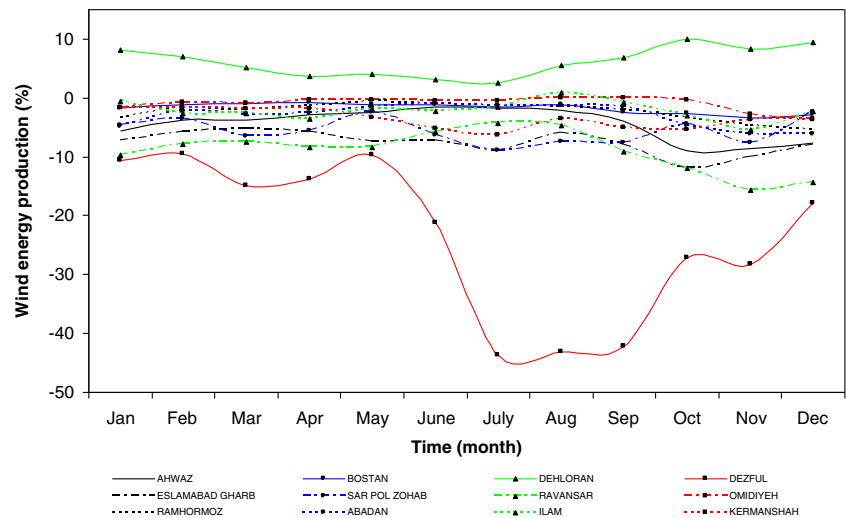


Fig. 13 Increment of wind energy production in the A1b scenario



Once the expected temperature, in accordance with the A2 scenario, was defined, its expected moist air density and wind energy production were obtained, as can be seen in Figs. 15 and 16. From Fig. 15, it can be concluded that moist air density will experience a reduction of 1 % in most of the cities, except in the city of Dehloran. The moist air in this region will experience an increment in density of 2 %, as a consequence of the lower temperature and high relative humidity.

In Fig. 16, the main consequences of this effect are shown. In agreement with the A1b scenario, wind energy production will increase by about 10 % in Dehloran. There is a clear decrement in wind energy production when it is compared with the A1b scenario. In Fig. 16, the maximum decrement in wind energy production was obtained in Dezful City, with values lower than a decrement of 40 %. This is due to the climate change effect that will cause a high increment of moist

air temperature and, under a low relative humidity, will yield very low wind energy output.

Conclusions

With respect to the significance of renewable energies and risk management in the field of energy, this research has focussed on the capacity of wind energy production in the southwestern and western regions of Iran. Different parameters, such as simulation of temperature measures via GCM models, predicting relative humidity by using the artificial neural network, preparing a wind speed profile for a height 65 m above ground level, calculating moist air density and finally calculating the capacity of wind energy production and comparing it with the present condition have all been taken into account. In any case, the results of this research indicate the

Fig. 14 Average future temperature in the A2 scenario

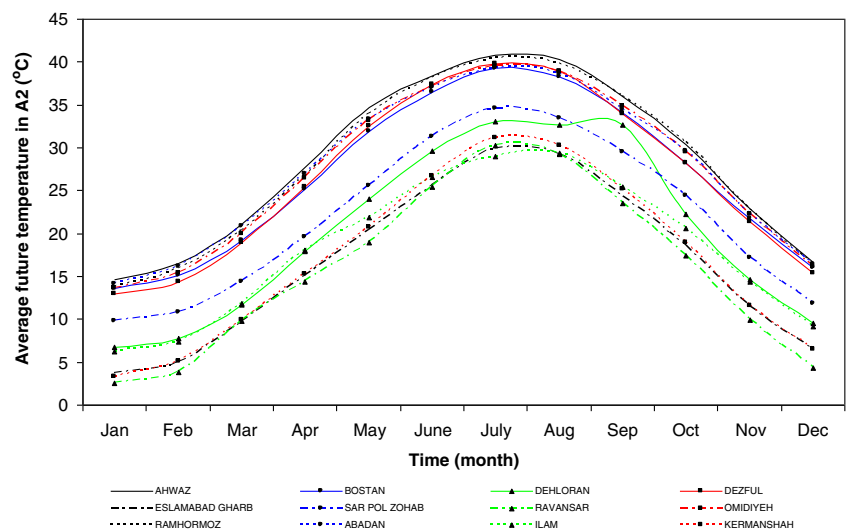
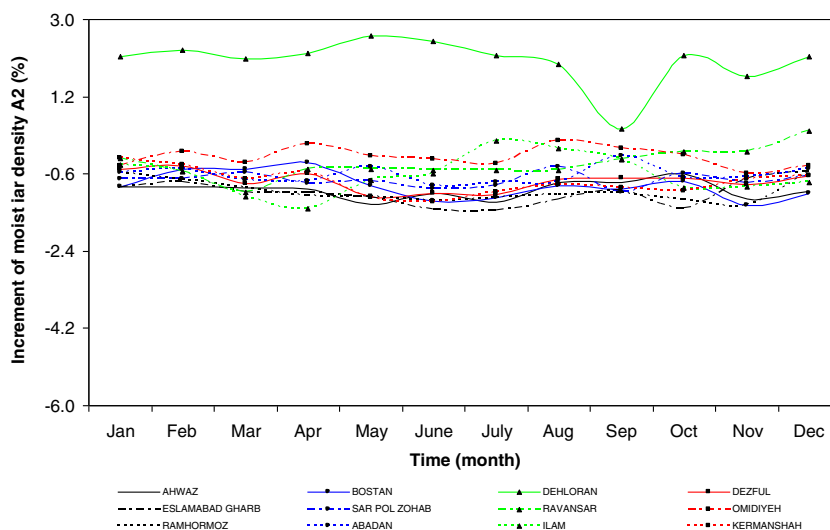


Fig. 15 Increment of moist air density in the A2 scenario (%)



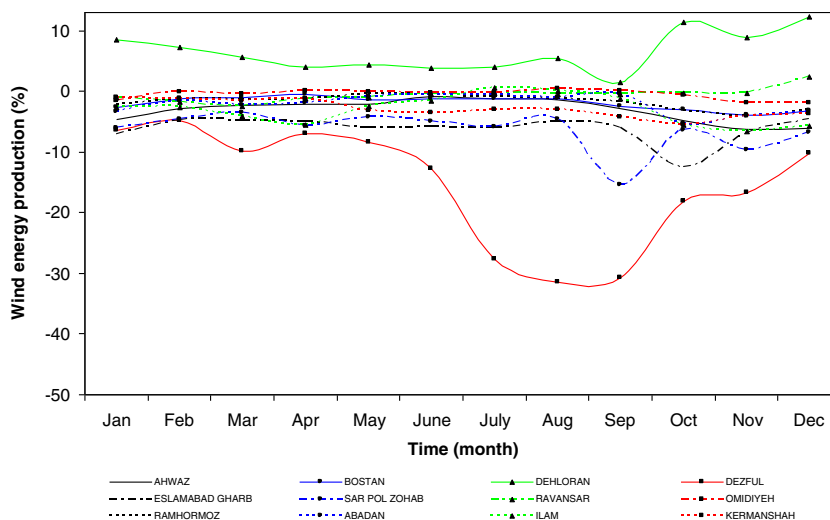
acceptable validity of the LARS-WG model and neural networks in simulating the parameters of temperature and relative humidity.

From Figs. 10 and 11, it can be concluded that there is an agreement between the two future climate scenarios of temperature, A1b and A2. In both simulations, Dehloran City shows the highest moist air density and consequently the highest wind energy production. In the other cities, a decrement of wind energy production is seen. Finally, if we consider that the mean working life of a real wind farm is between 20 and 30 years, we can choose regions with a greater potential in Iran, to implement and/or renovate wind farms, in accordance with the expected future wind energy production. Besides, many more research studies must be developed based on this new methodology.

As the temperature data output for the future decades show, taking into account global warming, the temperature will increase in all the studied regions. On the other hand, based on the A1b scenario and considering

the future climate change, the results indicate a decrease in the output capacity of wind energy production in almost all the cities. As the results show, the maximum measure of temperature will also occur in summer, and it is calculated that the highest decrease in wind energy production will be in the same season. Therefore, considering the increase in temperature and the decrease in the potential of wind energy production in the future decades, it could be concluded that the studied regions, particularly the Khuzestan province, will be faced with severe challenges in the field of energy supply for the cooling and ventilation of buildings. Thus, in order to manage this condition, a search must be implemented, for alternative and clean sources of energy, which not only do not exacerbate the conditions of global warming in the region but are also easily and abundantly accessible. Therefore, considering the potential of the region, due to exposure to sunlight, there must be more studies in the field of harnessing and utilising solar energy.

Fig. 16 Wind energy production in the A2 scenario (%)



References

- AL-Yahyaia S, Charabib Y, Gastlia A, Al-Alawia S (2010) Assessment of wind energy potential locations in Oman using data from existing weather stations. *Renew Sustain Energy Rev* 14:1428–1436
- AL-Yahyaia S, Roshan Gh, Ghanghermeh A (2014) Wind resource assessment over Iran using weather station data. *Int J Sustain Energy* doi: 10.1080/14786451.2014.885028
- Alamdari P, Nematollahi O, Mirhosseini M (2012) Assessment of wind energy in Iran: a review. *Renew Sustain Energy Rev* 16:836–860
- Awadh SM, Ahmad LMR (2012) Climatic prediction of the terrestrial and coastal areas of Iraq. *Arab J Geosci* 5:465–469
- ASHRAE (1988) Handbook. HVAC Fundamentals Editorial Index, Atlanta
- Babaeian I, Kwon WT (2005) Climate change assessment over Korea using stochastic daily data. Proceeding of the First Iran–Korea Joint Workshop on Climate Modeling, Nov. 2005. Climate Research Institute, Mashad
- Coulibaly P, Anctil F, Bobe B (2000) Daily reservoir inflow forecasting using artificial neural networks with stopped training approach. *J Hydrol* 230:244–257
- Choobasti AJ, Farrokhsad F, Barari A (2009) Prediction of slope stability using artificial neural network (case study: Noabad, Mazandaran, Iran). *Arab J Geosci* 2:311–319
- Dehghan A (2011) Status and potentials of renewable energies in Yazd Province-Iran. *Renew Sustain Energy Rev* 15:1491–1496
- Energy Information Administration (EIA) (2009) website www.eia.doe.gov/iea.
- Fadaia D, Esfandabadi Z, Abbasic A (2011) Analyzing the causes of non-development of renewable energy-related industries in Iran. *Renew Sustain Energy Rev* 15:2690–2695
- Frankovic B, Vrsalovic I (2001) New high profitable wind turbines. *Renew Energy* 24:491–499
- Ghorashi A, Rahimi A (2011) Renewable and non-renewable energy status in Iran: art of know-how and technology-gaps. *Renew Sustain Energy Rev* 15:729–736
- Huang J, Jinming G, Weng F (2007) Detection of Asia dust storms using multi sensor satellite measurements. *Remote Sens Environ* 110: 186–191
- Hu Z, Wang J, Byrne J, Kurdgelashvili L (2013) Review of wind power tariff policies in China. *Energy Policy* 35:41–50
- Keyhani A, Ghasemi-Varnamkhasti M, Khanali M, Abbaszadeh R (2010) An assessment of wind energy potential as a power generation source in the capital of Iran, Tehran. *Renew Sustain Energy Rev* 35:188–201
- Hojati S, Khademi H, Faz Cano A, Landi A (2011) Characteristics of dust deposited along a transect between central Iran and the Zagros Mountains. *Catena* J 88:27–36
- Iqbal MJJ, Quamar MA, Yousufzai K (2011) Spectral analysis of local climatic fluctuations. *Arab J Geosci* 4:291–298
- Johnson GL, Hanson CL, Hardegree SP, Ballard EB (1996) Stochastic weather simulation: overview and analysis of two commonly used models. *J Appl Meteorol* 35:1878–1896
- Meibom P, Weber C, Barth R, Brand H (2009) Operational costs induced by fluctuating wind power production in Germany and Scandinavia. *IET Renew Power Gen* 3:75–83
- Mirhosseini M, Sharifi F, Sedaghat A (2011) Assessing the wind energy potential locations in province of Semnan in Iran. *Renew Sustain Energy Rev* 15:449–459
- Mostafaeipour A (2010) Feasibility study of offshore wind turbine installation in Iran compared with the world. *Renew Sustain Energy Rev* 14:1722–1743
- Mostafaeipour A, Sedaghatb A, Dehghan-Niric AV, Kalantarc V (2011) Wind energy feasibility study for city of Shahrabak in Iran. *Renew Sustain Energy Rev* 15:2545–2556
- MeteoGalicia. “Galicia Climatic Data 2007” (2007) Consellería de Medio Ambiente. Xunta de Galicia. 1–124.
- Najafi G, Ghobadian B (2011) Wind energy resources and development in Iran. *Renew Sustain Energy Rev* 15:2719–2728
- Najafi MS, Khoshakhlagh F, Zamanzadeh SM, Shirazi MH, Samadi M, Hajikhani S (2013) Characteristics of TSP loads during the Middle East Springtime Dust Storm (MESDS) in Western Iran. *Arab J Geosci* doi:10.1007/s12517-013-1086-z
- Oil and Gas Journal, as of January .(2010). <http://www.ogj.com/index.html>.
- Petersen EL, Mortensen NG, Landberg L, Højstrup J, Helmut F (1997) Wind power meteorology. Riso National laboratory, Denmark [Riso-1-1206(EN)]
- Roshan GR, Ranjbar F, Orosa JA (2010) Simulation of global warming effect on outdoor thermal comfort conditions. *Int J Environ Sci Technol* 7:571–580
- Roshan GR, Khoshakh Lagh F, Azizi G, Mohammadi H (2011) Simulation of temperature changes in Iran under the atmosphere carbon dioxide duplication condition, Iran. *J Environ Health Sci Eng* 9:139–152
- Roshan Gh R, Grab S (2012) Regional climate change scenarios and their impacts on water requirements for wheat production in Iran. *Int J Plant Prod* 6:239–265
- Roshan GR, Ghanghermeh AA, Nasrabadi T, Bahari Meimandi J (2013a) Effect of global warming on intensity and frequency curves of precipitation, case study of Northwestern Iran. *Water Resour Manag*. doi:10.1007/s11269-013-0258-7
- Roshan G, Ghanghermeh A, Orosa JA (2013b) Thermal comfort and forecast of energy consumption in Northwest Iran. *Arab J Geosci*. doi:10.1007/s12517- 013-0973-7
- Roshan GHR, Oji R, Al-Yahyai S (2013c) Impact of climate change on the wheat-growing season over Iran. *Arab J Geosci*. doi:10.1007/s12517-013-0917-2
- Sabzevan A (1977) Performance characteristics of concentrator augmented Savonius wind rotors. *Wind Eng* 1:198–20
- Shikha T, Bhatti S, Kpithari DP (2003) A new vertical axis wind rotor using convergent nozzles. *Large Eng. Conference on Power Eng* 177–181.
- Shikha T, Bhatti S, Kothari DP (2005) Air concentrating nozzles: a promising option for wind turbines. *Int J Energy Technol Policy* 3: 394–412
- Semenov MA, Brooks RJ, Barrow EM, Richardson CW (1998) Comparison of the WGEN and LARS-WG stochastic weather generators in diverse climates. *Clim Res* 10:95–107
- Semenov MA, Barrow EM (1997) Use of a stochastic weather generator in the development of climate change scenarios. *Climate Change* 35: 397–414
- Semenov MA (2007) Developing of high-resolution UKCUP02-based climate change scenarios in the UK. *Agric Forest Meteorol* 144: 127–138. doi:10.1016/j.agrformet.2006.01.002
- World Wind Energy Report 2009 (WWEA). Date of publication: March 2010.06.30, <http://www.wwindea.org/home/index.php>, www.wweec 2010.com.
- Xu YP, Zhang X, Tian Y (2012) Impact of climate change on 24-h design rainfall depth estimation in Qiantang River Basin, East China. *Hydrol Process*. doi:10.1002/hyp.9210
- Zare Abyaneh H, Ghasemi A, Bayat varkeshi M, Marofi S (2009) Assessment of artificial neural network (ANN) in prediction of garlic evapotranspiration (ETC) with lysimeter in Hamedan. *J Water Soil* 23:176–185
- Zarghami M, Abdi A, Babaeian I, Hassanzadeh Y, Kanani R (2011) Impacts of climate change on runoffs in East Azerbaijan, Iran. *Glob Planet Chang* 78:137–146